Provided for non-commercial research and education use.
Not for reproduction, distribution or commercial use.

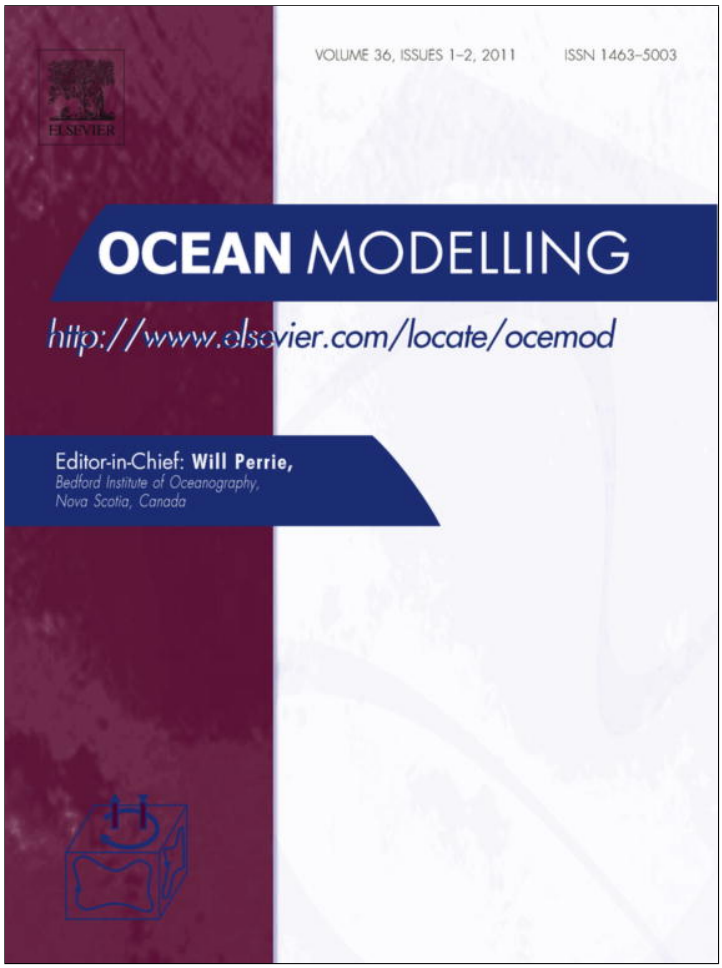

This article appeared in a journal published by Elsevier. The attached copy is furnished to the author for internal non-commercial research and education use, including for instruction at the authors institution and sharing with colleagues.

Other uses, including reproduction and distribution, or selling or licensing copies, or posting to personal, institutional or third party websites are prohibited.

In most cases authors are permitted to post their version of the article (e.g. in Word or Tex form) to their personal website or institutional repository. Authors requiring further information regarding Elsevier's archiving and manuscript policies are encouraged to visit:

http://www.elsevier.com/copyright

Author's personal copy

Ocean Modelling 36 (2011) 133–148

Contents lists available at ScienceDirect

Ocean Modelling

journal homepage: www.elsevier.com/locate/ocemod

How does the Red Sea outflow water interact with Gulf of Aden Eddies?

Mehmet Ilıcak [a,*], Tamay M. Özgökmen [b], William E. Johns [b]

[a] Princeton University, AOS, NJ, USA
[b] RSMAS, 4600 Rickenbacker Causeway, Miami, FL 33149, USA

ARTICLE INFO

Article history:
Received 13 August 2010
Received in revised form 22 September 2010
Accepted 28 October 2010
Available online 10 November 2010

Keywords:
Red Sea overflow
Gulf of Aden eddies
Gravity current
Mixing

ABSTRACT

As the Red Sea overflow water (RSOW) enters the Gulf of Aden (GOA), it interacts with a sequence of nearly barotropic, mesoscale eddies originating in the Indian Ocean. To investigate how these eddies impact the dispersal and eastward transport of the RSOW toward the Indian Ocean, a high resolution 3D regional model is employed to explore systematically the interaction between the RSOW and mesoscale eddies. Two types of experiments are conducted. In the first set, we simulate the behavior of RSOW in the presence of an idealized cyclone and an idealized anticyclone. The second type of simulation involves nesting of the regional model (ROMS) within a data-assimilating global model (HYCOM), in which a sequence of mesoscale eddies entering the Gulf of Aden is realistically captured. This simulation is integrated for one year, and includes a simple representation of the seasonality of the RSOW.

Bower et al. (2002) suggest that the Red Sea overflow might be a western boundary undercurrent. Consistent with these expectations, the idealized simulations show that the preferred pathway of the RSOW in the absence of eddies is along the coast of Somalia (southern continental shelf) as a western boundary undercurrent. Simultaneously, a cyclonic circulation is generated in the far western GOA due to vortex stretching by the descending outflow. The presence of a cyclone in the western GOA increases the peak RSOW transport, but the cyclone itself rapidly loses its coherence after interacting with the rough topography in the western GOA. The presence of an anticyclone tends to block the preferred boundary pathway and inhibits the eastward transport of the RSOW. The eddies also result in substantially increased mixing of the RSOW in the western GOA.

On the basis of the more realistic ROMS experiment, it is found that the modeled RSOW leaves the western part of the Gulf of Aden in short episodic bursts with transports that are an order of magnitude greater than that associated with the quasi-steady RSOW inflow into GOA. Such enhancement in RSOW transport is shown to be induced by cyclonic eddies that cause a rapid discharge of RSOW from the western part of the GOA. We conclude that mesoscale eddies play a key role in the transport and mixing of the RSOW within GOA.

© 2010 Elsevier Ltd. All rights reserved.

1. Introduction

Saline, dense Red Sea deep water is formed in the northern Red Sea due to excessive evaporation and exits the Red Sea as a dense overflow through the Bab al Mandeb strait (Murray and Johns, 1997; Morcos, 1970). As it enters the western Gulf of Aden (GOA), it divides into two channels: a very narrow (~5 km wide), long northern channel and a broader, shorter southern channel (Bower et al., 2005; Peters et al., 2005). It then reaches neutral buoyancy at different depths in the western GOA and spreads laterally through the Gulf. According to observations, the Red Sea outflow becomes a major intermediate water mass in the Indian Ocean (Beal et al., 2000). The properties of this water mass are modified by the mixing and stirring processes that take place in the GOA (Bower et al., 2005). Although the annual mean volume transport of the Red Sea overflow water (≈0.37 Sv where $1\ \text{Sv} \equiv 10^6\ \text{m}^3/\text{s}$) is relatively small compared to major overflows such as the Mediterranean overflow (≈1 Sv) or the Denmark Strait overflow (≈2.9 Sv) (Murray and Johns, 1997; Candela, 2001; Girton et al., 2001; Macrander et al., 2007), it has a distinctive and far reaching signal. The Red Sea overflow water has been observed as far as the Agulhas Current (Roman and Lutjeharms, 2007), from which it seems to be transported to the South Atlantic.

Modeling of the Red Sea overflow is a challenging problem because of demands on resolution to be fine enough to resolve the channels and accuracy of mixing parameterizations. There are only few studies in which it was attempted to model the Red Sea outflow. Özgökmen et al., 2003 and Ilıcak et al., 2008b used 2D non-hydrostatic models to reproduce the Red Sea gravity current in the northern channel. Chang et al., 2008 and Ilıcak et al., 2008a

* Corresponding author. Address: Mehmet Ilıcak. 201 Forrestal Road Princeton, NJ 08540, USA. Tel.: +1 7863251094.
E-mail addresses: milicak@princeton.edu, milicak@rsmas.miami.edu (M. Ilıcak).

1463-5003/$ - see front matter © 2010 Elsevier Ltd. All rights reserved.
doi:10.1016/j.ocemod.2010.10.006

Author's personal copy

modeled the Red Sea overflow using different mixing parameterizations in 3D hydrostatic models and conducted a detailed comparison with data from the 2001 Red Sea Overflow Experiment (REDSOX). In Fig. 1, the bottom layer salinity field is shown from one of our simulations. It can be seen that the northern channel carries most of the overflow, consistent with observations that show that the northern channel transports about two-thirds of the total Red Sea overflow (Matt and Johns, 2007). The total Red Sea Overflow Water (RSOW) transport is around 0.56 Sv at the exit of the channels, where the dense plumes separate from the bottom at the edge of the Tadjura Rift (Fig. 1). The two branches of the overflow equilibrate at different depths in the western GOA; around 800 m for the northern channel flow, and around 550 m for the southern channel flow. Peters et al., 2005 defined two distinct layers to describe the vertical structure of the descending overflow in the channels, a bottom layer (BL), and an overlying interfacial layer (IL). The former reaches from the bottom to a height where the velocity is maximum, and the latter extends from this maximum upward with strong stratification and large shear. The BL is well-mixed and maintains high salinities along the northern channel. In contrast, the IL shows stronger entrainment and carries most of the overall plume transport, increasingly so with downstream distance. However, previous numerical studies have focused on accurate modeling of the Red Sea overflow in a limited basin and excluded any consideration of what happens to the RSOW beyond the Tadjura Rift.

The surface circulation in the GOA is dominated by seasonal wind forcing and a series of mesoscale eddies (Fratantoni et al., 2006; Al Saafani et al., 2007). The size of these eddies can be as large as the width of the Gulf (~200 −300 km) and their azimuthal speed can be as high as 0.5 m/s (Fig. 2). Bower et al., 2002 find that the cyclonic and anticyclonic eddies are in fact nearly barotropic and can reach as deep as 1500 m.

There are different theories for the generation of GOA eddies. Fratantoni et al. (2006) described the passage of a series eddies into the Gulf mostly during the transition between summer and winter monsoons. They showed that the dominant mechanism for these eddies are the instabilities and retroflection of the Somali Current due to monsoon winds. Al Saafani et al. (2007) showed that some of the eddies also propagate into the GOA from the Arabian Sea. The dynamics of these eddies involve interactions with westward propagating Rossby waves generated in the Indian Ocean by poleward propagating Kelvin waves during the winter monsoon (Al Saafani et al., 2007).

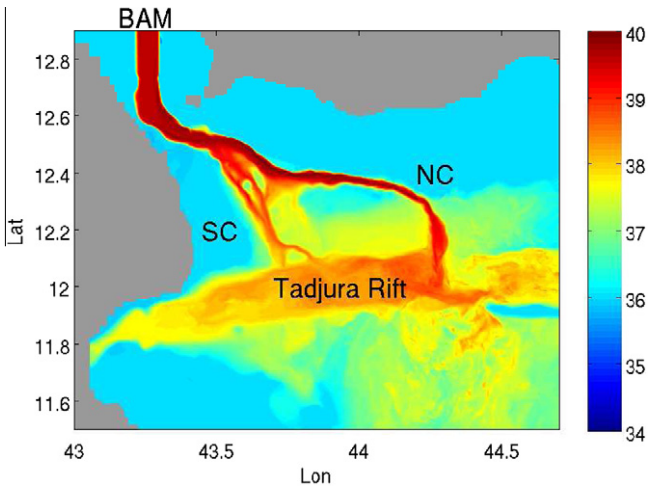

Fig. 1. Maximum salinity [psu] values in the whole water column at time = 120 days. The overflow has separated into the northern and the southern channels. BAM = Bab al Mandeb, NC = Northern Channel, SC = Southern Channel. The overflow splits into two at Lat ≈12.4°N and both plumes separate from the bottom at the Tadjura Rift.

Even though these eddies are now relatively well documented, their effect on the RSOW remains unknown. Aiki et al., 2006 employed a 3D global ocean circulation model to understand characteristics of the Red Sea outflow in the GOA. Their model resolution was not high enough to capture the channels, hence all of the outflow followed the northern channel only. Since the southern channel is not included in that model, they did not simulate the multilayer structure of the Red Sea overflow in the GOA. Aiki et al., 2006 found that the discharged Red Sea outflow and incoming Indian Ocean intermediate water are characterized by anticyclonic and cyclonic circulation, respectively.

In this paper, we study the interaction between the RSOW and GOA eddies. Our objective is to address the following questions:

(a) How is the RSOW transported through the mesoscale eddy field in the Gulf of Aden?
(b) Is there a preferred pathway of the Red Sea overflow out of Gulf of Aden?
(c) Do the eddies act to homogenize the RSOW? If not, how do they influence the fate of this overflow?

Since the interaction between the overflow and multiple eddies can be complex, we start with a simplified problem, and then progress to a more realistic setting. We first consider the overflow in the absence of any eddies in the GOA. After that, an idealized cyclone or anticyclone is initialized with the overflow in two cases. Our focus is on the pathway of the overflow in the presence of an idealized eddy. We then move to a more realistic simulation using a global ocean circulation model including multiple, propagating eddies in the GOA. The overflow transport and mixing in different simulations are also computed for quantitative analysis. To our knowledge, this is the first time that a set of detailed and systematic numerical simulations have been conducted to understand the interaction between the Red Sea overflow and GOA eddies.

Our main finding is that GOA eddies can modulate the transport of RSOW significantly such that RSOW leaves the western half of the GOA in short episodic burst with transports reaching 6 Sv, which is an order of magnitude larger than the steady transport of RSOW out of the channels. Such enhancement of the RSOW transport within the GOA is shown to be induced by cyclonic GOA eddies, while anticyclonic eddies tends the block the eastward propagation of the RSOW. GOA eddies have speeds comparable to RSOW during its descent from the Bab al Mandeb (BAM) Strait. Cyclonic eddies propel RSOW eastward by acting over a much larger cross-sectional area when compared to that of the BAM, resulting in a rapid discharge of RSOW from the western part of the GOA.

This paper is organized as follows: The numerical model and setup of the numerical experiments are introduced in Section 2. The main results are presented in Sections 3 and 4 for idealized and realistic simulations, respectively. We provide a discussion on the time-varying export of RSOW from the western Gulf of Aden and the enhanced growth of the RSOW transport caused by the eddies in Section 5. Finally, we summarize and conclude in Section 6.

2. Model setup

In this study, Regional Ocean Modeling System (ROMS) is chosen as the numerical model. ROMS is a free-surface, hydrostatic, primitive equations ocean model that uses orthogonal curvilinear horizontal coordinates on an Arakawa C grid. The primitive equations are discretized over topography in the vertical using stretched terrain-following, or "sigma", coordinates (Shchepetkin and McWilliams, 2005). The model domain covers the area

Author's personal copy

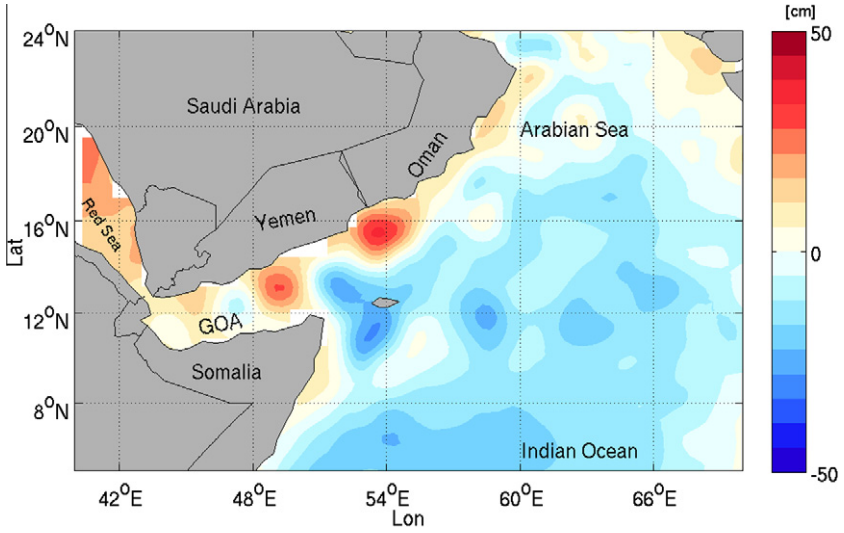

Fig. 2. Sea surface height (SSH) anomaly for the GOA and Arabian Sea on January 6, 1999, from AVISO (`http://www.aviso.oceanobs.com`). Several GOA eddies are evident (red = anticyclones, blue = cyclones) with SSH anomalies of up to 25 cm. (For interpretation of the references to color in this figure legend, the reader is referred to the web version of this article.)

between longitude 43°E and 48°E, latitudes 10.2°N and 13°N (Fig. 3(a)). The domain is an extended version of the domain of Ilıcak et al., 2008a (henceforth IL08). IL08 carefully studied the Red Sea overflow with different vertical turbulence closures and compared model results to the observations. They concluded that two-equation turbulence closures perform well with high-resolution provided that forcing and initial conditions are correct. Therefore, the same initial conditions and forcing of the overflow from IL08 are employed in this study. We also use $k-\varepsilon$ turbulence closure with Canuto-B (Canuto et al., 2001) stability functions for the vertical mixing scheme. A nonuniform grid resolution is used in the model with the horizontal grid spacing changing from 250 m to 450 m until 46°E, and after that grid resolution gradually coarsens to 10 km toward the end of the domain (Fig. 3(b)). This was necessary to use open boundary conditions effectively in the east and north sides of the domain. The vertical resolution relies on 30 sigma layers, unevenly spaced and clustered near the bottom and intermediate level of the water column since the major interest is in these areas.

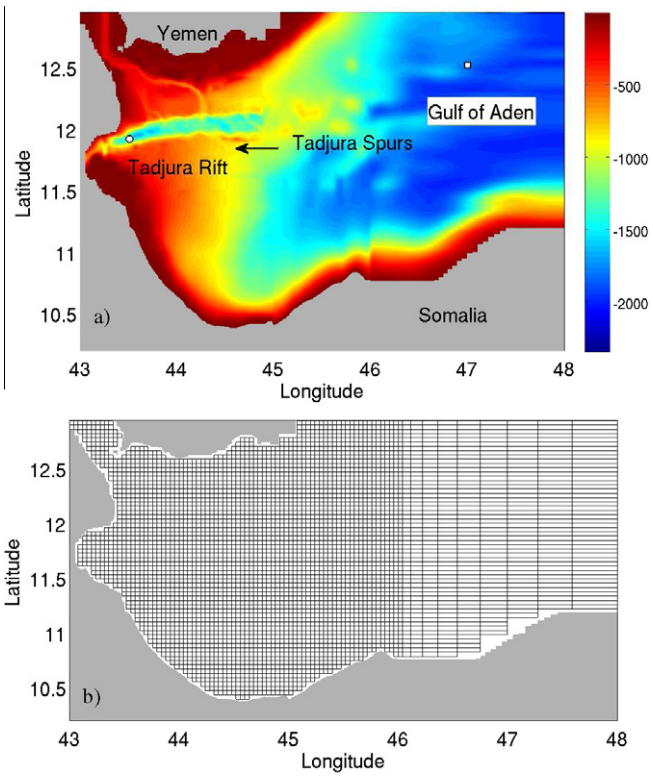

Fig. 3. (a) Gulf of Aden bathymetry in [m] and idealized eddy location (red circle). (b) Model grids in every 10 points until 46°E and in every 5 points after that. (For interpretation of the references to color in this figure legend, the reader is referred to the web version of this article.)

According to observations performed in 2001 Red Sea Outflow Experiment (REDSOX), water properties (temperature and salinity) of the east and west side of the Gulf of Aden are different. Therefore, the model domain is initialized by temperature (T) and salinity (S) profiles from two different REDSOX stations; one is in the Tadjura Rift (circle dot in Fig. 3(a)), the other is in the Gulf of Aden away from the Tadjura Rift (square dot in Fig. 3(a)). The profiles from these stations are projected to the local water depth at any other location. Dense overflow water is introduced into the domain as follows. At the north-western side of the domain, dense water representing the overflow coming from Bab al Mandeb Strait is released. T/S profiles in this area are relaxed towards profiles taken from the REDSOX observations in the Bab al Mandeb Strait. The Red Sea overflow is mainly a salinity-driven outflow, hence all the following discussions are based only on the salinity field.

A nonlinear equation of state (Jackett and McDougall, 1995) is used to compute density. Open boundary conditions (Marchesiello et al., 2001) are employed at the eastern boundary. Once the dense water is released from the BAM Strait, the model is integrated for 120 days. Wind forcing as well as evaporation, precipitation and radiative heat fluxes are set to zero everywhere. A quadratic bottom drag formulation with a drag coefficient of $C_d = 5 \times 10^{-3}$ is used to incorporate the bottom shear stress. The parameters specified above have been tested in Ilıcak et al., 2008a. All experiments are performed with $800 \times 702 \times 30$ grid points in x, y, and z directions, respectively. The baroclinic time step is set to 30 s, and 20 barotropic time steps are used between each baroclinic time step. The experiments are conducted on an IBM p-575 cluster. All idealized simulations are conducted on 64 processors and take approximately five days of wall clock time for an integration time of 120 days.

Author's personal copy

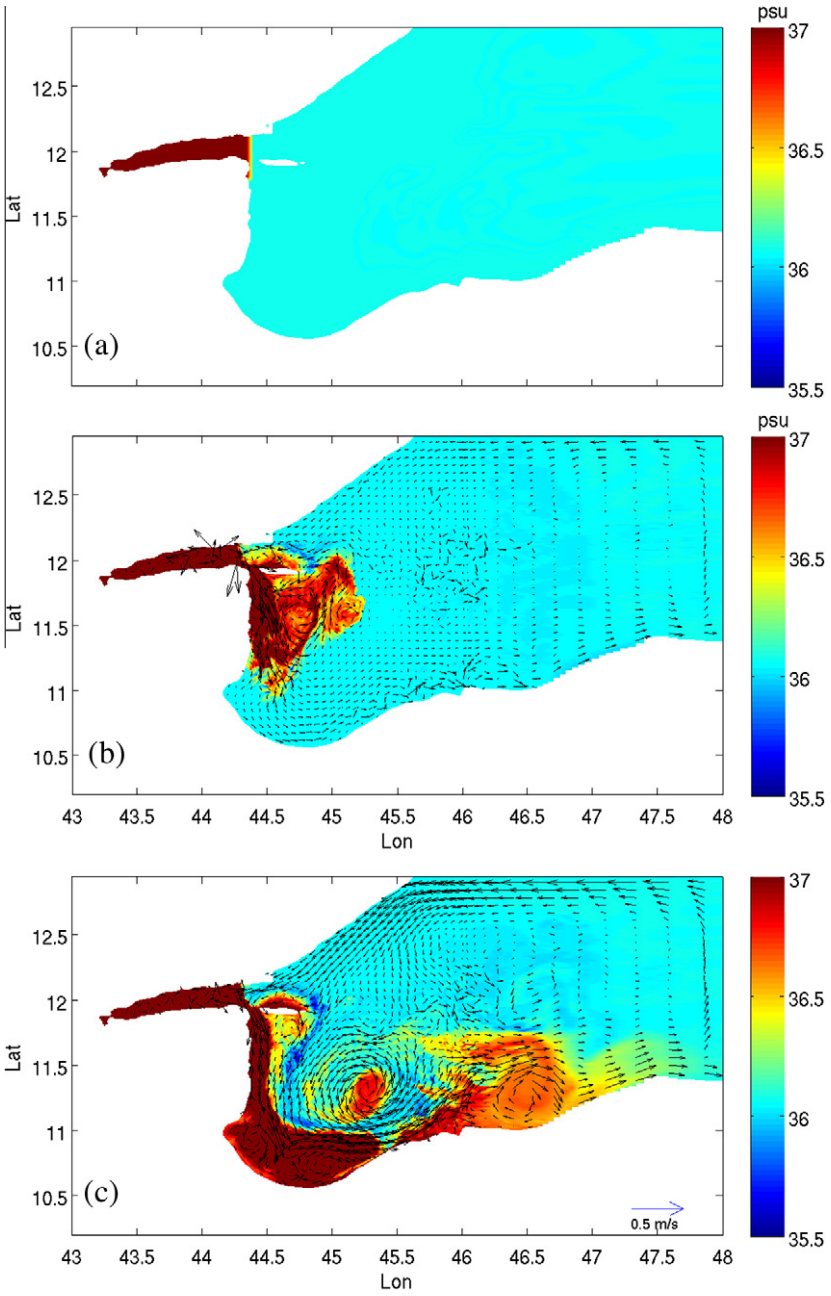

Fig. 4. Horizontal section for salinity field (color) and velocity vectors at $z = -800$ m for (a) case **O** at time = 0, (b) case **O** at time = 40, (c) case **O** at time = 120 days. (For interpretation of the references to color in this figure legend, the reader is referred to the web version of this article.)

3. Interaction of RSOW with idealized GOA eddies

3.1. Setup and list of experiments

The numerical experiments are organized as follows. The first part consists of idealized cases with various combinations of RSOW and GOA eddies. Three different experiments are conducted; overflow without any eddies (**O**), overflow with an idealized cyclone (**O + C**) and overflow with an idealized anticyclone (**O + A**). The second part of our investigation involves a realistic sequence of GOA eddies supplied through the eastern boundary of the regional domain from a data-assimilating global model.

Since satellite data show that westward propagation of Indian Ocean eddies into the Gulf takes months (Fig. 2), it is important for us to model an eddy that does not dissipate in a short amount of time. To simulate the GOA eddies, we employ an isolated (or shielded) barotropic vortex with initial velocity field at the form

$$v_\theta = A_0 \frac{r}{R} e^{-\frac{r^2}{R^2}}, \tag{1}$$

where v_θ is the tangential velocity, A_0 is the magnitude, r is the distance from the center of the eddy (Carton et al., 1989). This satisfies the necessary and sufficient condition for an isolated vortex that the area integral of the relative vorticity ($\zeta = \partial_x v - \partial_y u = \nabla^2 \psi$) vanishes at all depths (Morel et al., 1997). Thus, the vortex has zero total circulation in all horizontal planes. The parameters $A_0 = 1.1$ m/s and $R = 50$ km are selected in order to provide that the maximum velocity is around 0.5 m/s consistent with observed GOA eddies (Bower et al., 2002).

Author's personal copy

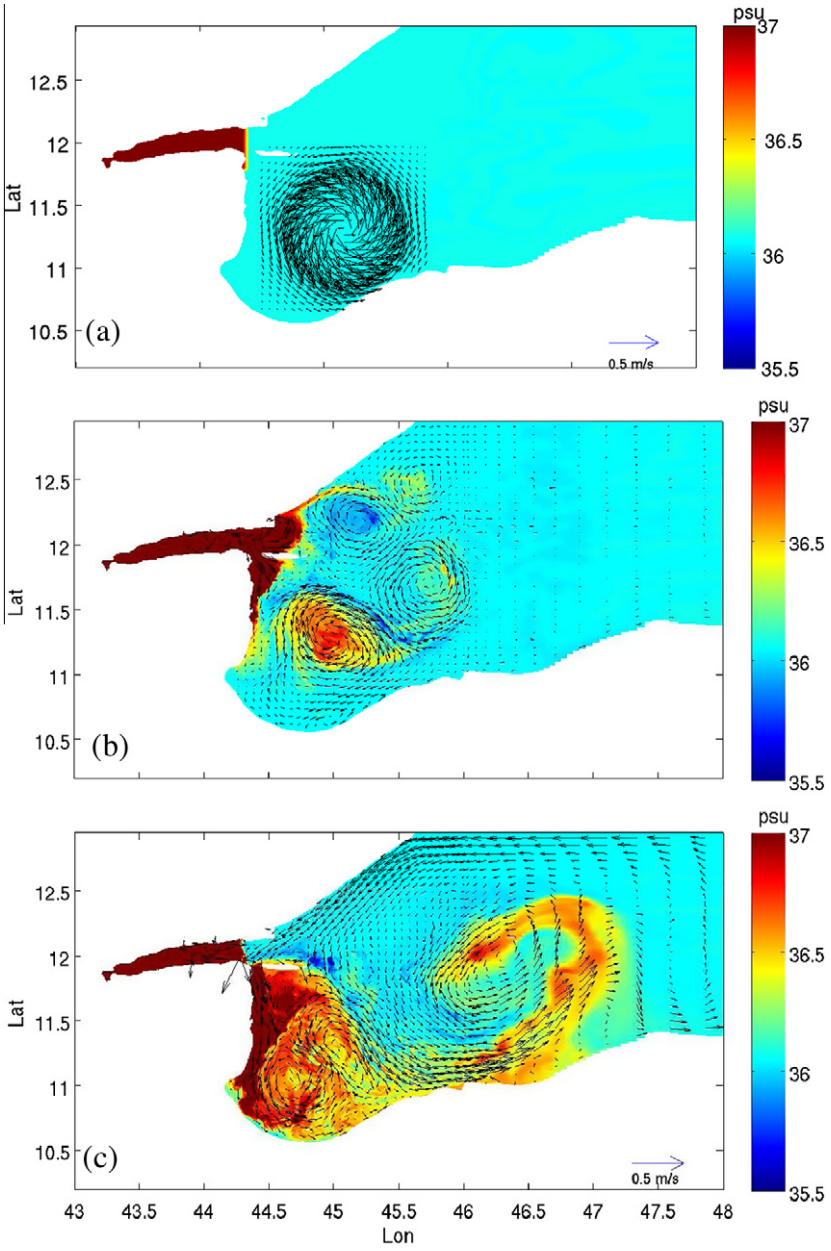

Fig. 5. Same as Fig. 4 but for the case **O + C**.

3.2. Pathways of RSOW

In the case **O**, the overflow is released in the absence of any eddies in the GOA domain. Initially, horizontal salinity section at 800 m displays two different water properties (Fig. 4(a)); one is saline water inside the Tadjura Rift (station 93) and the other is fresher water in the GOA (station 182). At time = 40 days, the overflow passes the Tadjura Spurs and a cyclone is formed just after the Spurs (Fig. 4(b)). Previous studies (Spall and Price, 1998; Ezer and Feb., 2006) also show cyclogenesis in the overflow systems due to potential vorticity (PV) conservation. Four months later, the cyclone generated by the overflow stays at the same location in the western part of the GOA (Fig. 4(c)). The overflow itself becomes an attached current that stays on the continental slope. Bower et al., 2002 expected that the Red Sea overflow might be a boundary undercurrent such as the Mediterranean outflow before they discovered the presence of eddies. The case **O** clearly shows that the Red Sea overflow follows the continental slope in the absence of GOA eddies.

In the case **O + C**, the overflow is released with an idealized cyclone in the GOA (Fig. 5(a)). One of the important mechanisms to transport the high salinity water is that it is encircled around the eddies and advected. At time = 120 days the initial cyclone has disappeared and the overflow has spread towards the western part of the GOA. There is a new cyclone around 44.7°E and 11.0°N. It seems that not only PV conservation but also arch-shaped topography favors the cyclone generation at the west side of the GOA (Fig. 5(c)). The overflow becomes attached on the shelf until 46°E and detaches from the boundary close to the east side of the numerical domain.

The third case **O + A** consists of the overflow and an idealized anticyclone in the GOA (Fig. 6(a)). After four months, the anticyclone still remains in the GOA. Even though some of the overflow filaments have encircled the anticyclone and been advected through it, most of the overflow water is trapped on the west side of the GOA. We do not see any saline water east of 46°E. The anticyclone stays at 45.6°E and acts like a barrier for the overflow water (Fig. 6(c)). Since the same amount of high saline water is

Author's personal copy

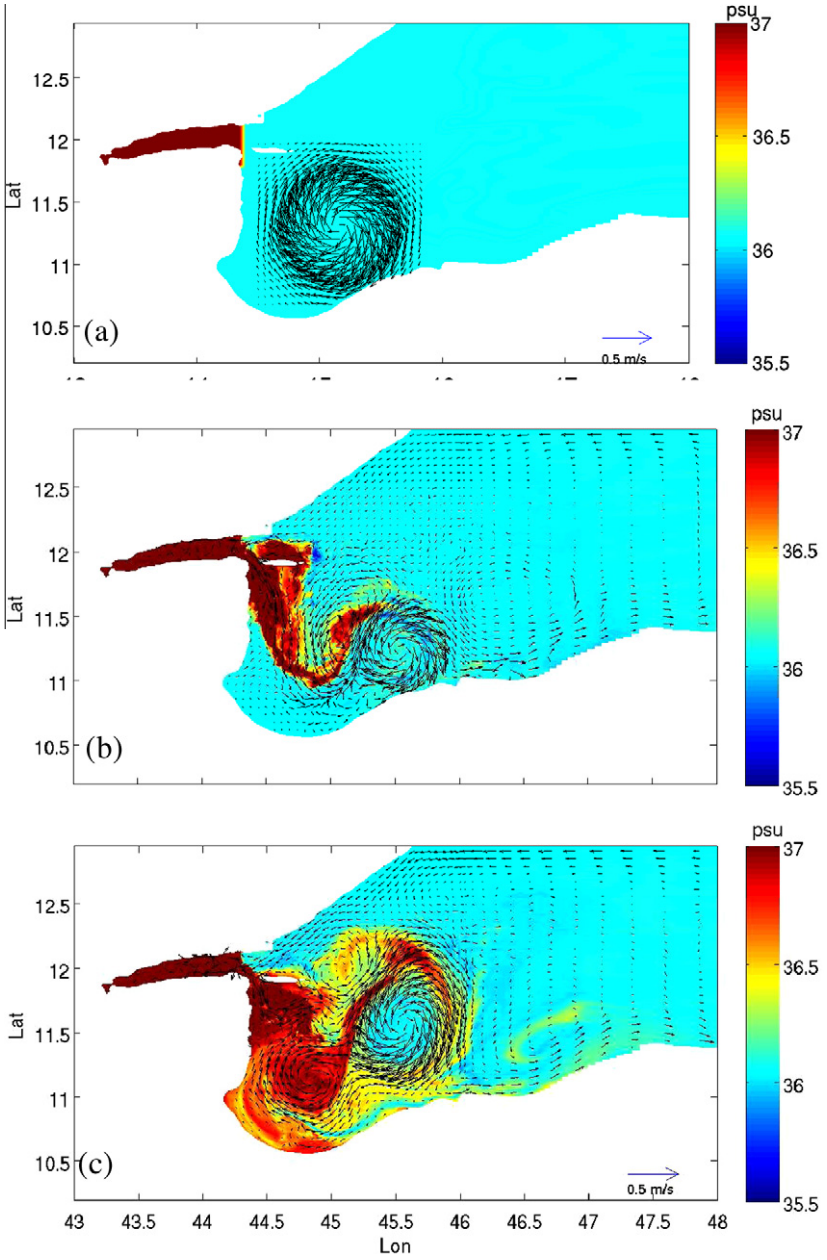

Fig. 6. Same as Fig. 4 but for the case **O + A**.

released from the north part of the domain at every time step (i.e. the source is constant) and the anticyclone traps the overflow into the west side, the overflow cannot go eastward, thus its pathway is changed. It is also clear that the overflow generates its own cyclone in all the idealized experiments. Furthermore, each of these cases results in a larger-scale cyclonic circulation, in which ambient GOA waters flow westward along the northern boundary of the basin to feed the actively entraining overflow plume, and the plume waters are exported preferentially along the southern boundary. This circulation is somewhat weaker in the **O + A** case since the initial anticyclone opposes it, but it can clearly be seen in all cases.

To look at the overflow structure in more detail, vertical sections at 45.75°E are plotted at time = 120 days (Fig. 7). Vertical section of the case **O** shows a distinct shelf-attached undercurrent on the south side of the domain (≈11°N). This current has two cores; one is around 500–550 m and the other is around 850–900 m (Fig. 7(a)). These cores are overflow waters coming from the southern and the northern channels. High salinity values (≈37 psu) that reach up to 12°N are a part of the cyclonic eddy generated by the overflow. For the **O + C** case (Fig. 7(b)), the shelf-attached under current can be also seen, however the current is rather thin compared to one in the previous case. The core of the current is equilibrated approximately around 950 m. The diluted RSOW occupying the interior of the section, up to 12.4°N, is derived from the coastal undercurrent after being wrapped around the cyclone in the southern GOA. In the case **O + A**, there is no undercurrent on the south side of the domain (Fig. 7(c)). Most of the overflow water is in the interior, having been advected around the anticyclone and then southward toward the southern boundary, where it is then swept westward back toward the outflow source. Both cases **O + C** and **O + A** tend to weaken the signature of the Red Sea outflow at the southern boundary and promote more vigorous mixing and stirring into the GOA.

Author's personal copy

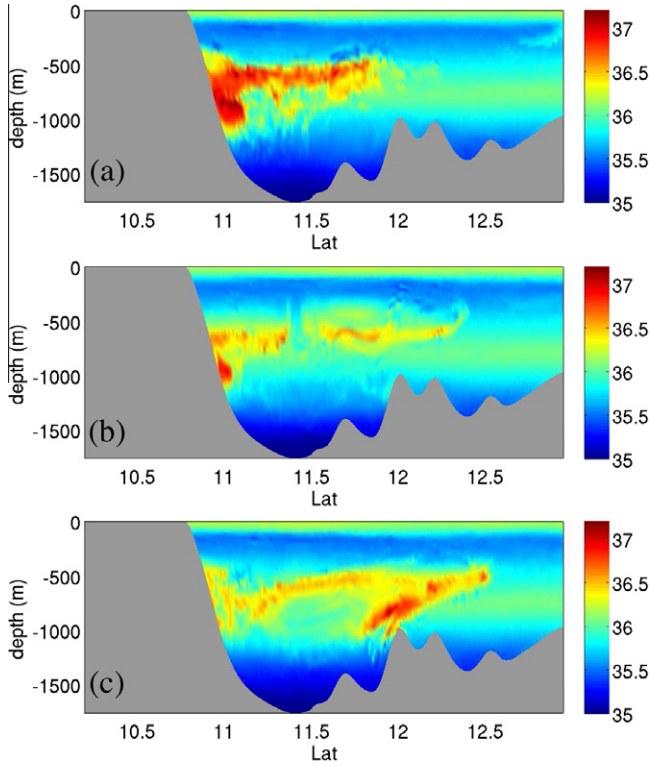

Fig. 7. Vertical sections for salinity field at Lon = 45.75°E for cases (a) **O**, (b) **O + C** and (c) **O + A**, respectively.

3.3. Transport and mixing

To quantify how much overflow water is leaving the domain in the different cases, we calculate the transport of RSOW at longitude 46°E, which lies the end of the high-resolution domain size and is a convenient location to measure the shelf-attached boundary current. We choose 36.5 psu as a threshold to define the Red Sea overflow water, as used in previous studies (Peters et al., 2005; Ilıcak et al., 2008b). Mass transport, $\int\int udzdy$, is computed at 46°E for 120 days (Fig. 8). In the base experiment, case **O**, for the first 70 days the transport is zero since there is no saline water larger than 36.5 psu that passes through 46°E. This means that the overflow has not yet arrived 46°E. After 70 days, the transport starts to increase and in 10 days it reaches a steady value of around 1 Sv. This is a reasonable number in comparison to observations. Peters et al., 2005 compute the Red Sea overflow transport as 0.7 Sv in the channels. The total volume in the numerical simulation for 120 days (i.e. the area under the transport line or the total volume that has exited 46°E) is 3.68×10^{12} m^3 (Table 1). In the case **O + C**, there are small and intermittent transport values at around 50 days. These transports are due to filaments advected by the cyclone and anticyclone as discussed before. After 80 days, the transport starts to increase linearly and reaches a maximum 1.72 Sv, before it drops to 1 Sv. Mean transport of the overflow (between 80 days and end of the simulation) is 0.9 Sv and the total volume is 2.66×10^{12} m^3. The transport in the last case **O + A** is different in comparison to the other cases. As shown in the previous section, the anticyclone acts as a barrier and does not let the overflow move to the east. Therefore the transport at 46°E is small; it is around 0.15 Sv and the total volume during the entire simulation time is only 0.6×10^{12} m^3. The total volume in the case **O + A** is 6.1 and 4.4 times lower than the total volume in cases **O** and **O + C**, respectively.

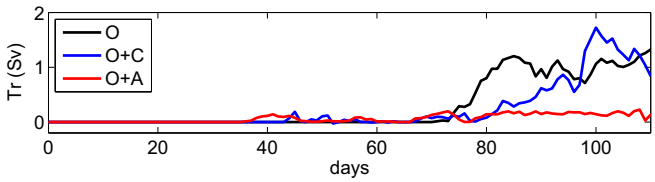

Fig. 8. Transport of the RSOW defined as $S > 36.5$ psu at 46°E for different cases.

To quantify the volume-averaged water properties in the domain, we look at the probability density function (pdf) of temperature-salinity (T/S) diagrams for the different cases. All the T/S profiles are used between 43°E and 46°E at time = 75 days since the overflow has not arrived at 46°E at this time in all cases (Fig. 8). Fig. 9(a) displays the initial pdf of the temperature and salinity in the model. The background stratification can be seen as the red line. High pdf value at $T = 14.5$ °C and $S = 37$ psu is due to the REDSOX station used for the initial condition. All grid points below 1000 m have the same water properties. Fig. 9(b) shows the pdf of the base experiment, **O**. Two cores of the overflow can be distinguished. Most of the overflow water are on the 37.4 and 37.6 isopycnic lines (green areas in Fig. 9(b)). These waters are saltier than 36.5 psu and warmer than 16 °C. However, in the idealized eddy experiments, greater mixing and dilution of the RSOW occurs. In the **O + C** case, most of the overflow water is fresher than 36.5 psu and colder than 16 °C (red lines in Fig. 9(c)). The **O + A** case is similar but results in slightly less overall mixing of the original RSOW than for the **O + C** case. This suggests that there is substantially increased lateral mixing of RSOW due to enhanced stirring and filamentation of the RSOW in the cases with eddies. These cases can be compared against the pdf of the temperature and salinity profiles obtained during the Red Sea Outflow Experiment cruise in winter 2001, during the season of maximum outflow (Fig. 9(e)). The reader is referred to Bower et al. (2002), Peters and Johns (2005), Bower et al. (2005), Peters and Johns (2006), Peters et al. (2005), Matt and Johns (2007) for the complete analysis of the observational results. All the stations west of 46°E are taken into account to compute the pdf. It is clearly seen that the observed pdf is similar to the pdfs in the modeled cases with GOA eddies. This is presumably due to the lateral mixing of the GOA eddies since Bower et al., 2002 observed two cyclones and an anti-cyclone during the REDSOX-I cruise. We conclude that interaction of the overflow with idealized eddies substantially enhances lateral mixing of the RSOW.

4. Interaction of RSOW with realistic GOA eddies

Finally, we consider the interaction between the Red Sea overflow and a realistic sequence of GOA eddies. An ocean general circulation model is required to use as an outer nest to provide synoptic mesoscale boundary conditions. The 1/12° Hybrid Coordinate Ocean Model (HYCOM) is employed since there is a global HYCOM simulation available between November 2003 to February 2009. Some information about the global HYCOM is as follows. The simulation was performed using a Mercator grid between 78°S and 47°N. A bipolar patch is used for regions north of 47°N. There are $4500 \times 3298 \times 32 = 474,912,000$ grid points in x, y and z, respectively. The Navy Operational Global Atmospheric

Table 1
Total Red Sea outflow water volume across 46°E for different experiments after 120 days of integration.

	O	**O + C**	**O + A**
Volume (m^3)	3.68×10^{12}	2.66×10^{12}	0.6×10^{12}

Author's personal copy

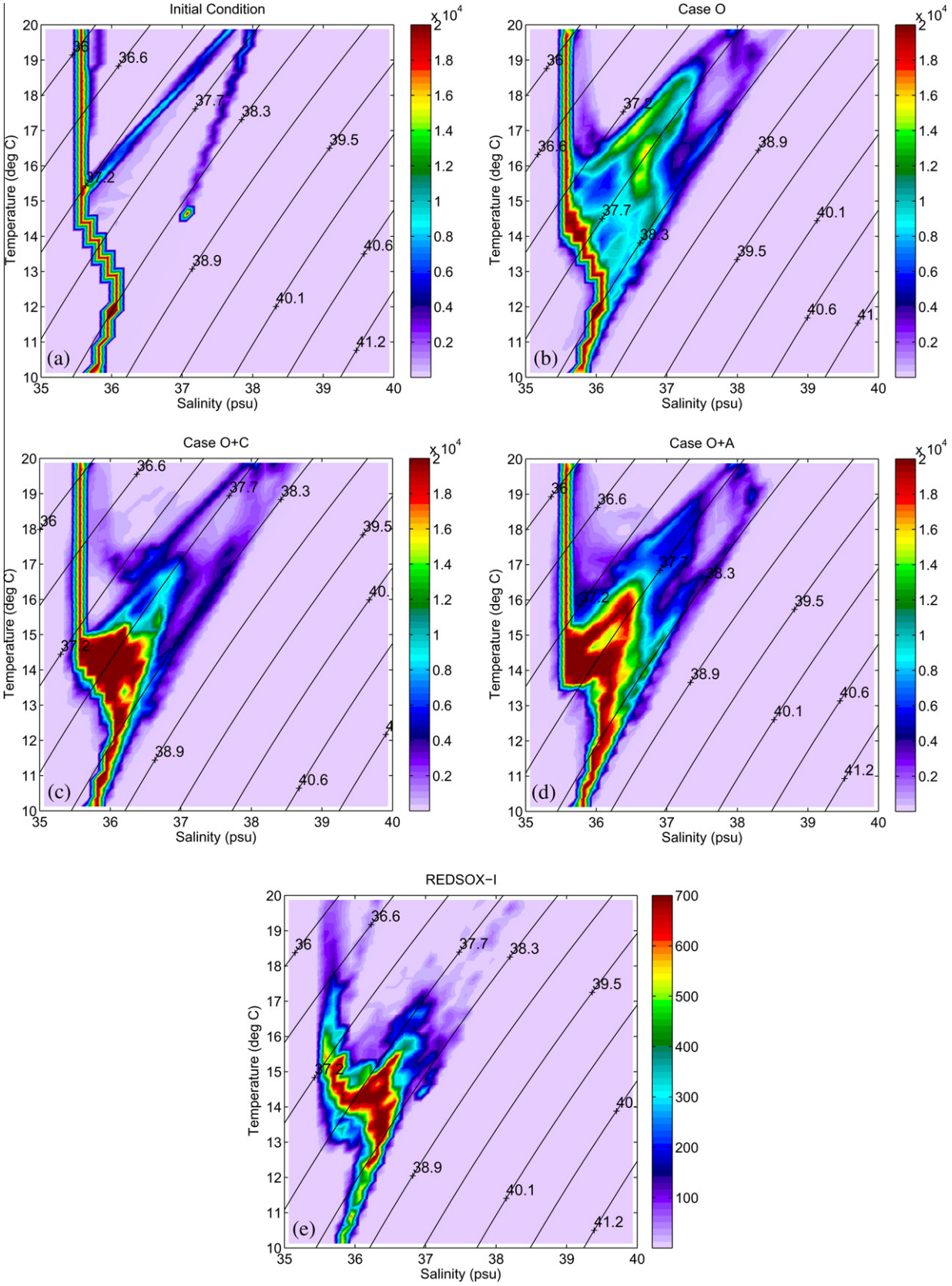

Fig. 9. Probability density function of the *T*/*S* diagrams between 43°E and 46°E: (a) for the model initial condition (b) for the case **O** (c) for the case **O + C** (d) for the case **O + A** (e) for the REDSOX-I hydrographic stations. Black contours are the σ_2 density lines computed at $z = 2000$ m.

Prediction System (NOGAPS) which includes wind stress, wind speed, heat flux, precipitation is used as surface forcing. This global run also uses the Navy Coupled Ocean Data Assimilation (NCODA) system (Cummings, 2005) for data assimilation. Although HYCOM

Author's personal copy

with NCODA data assimilation provides us realistic surface and deep circulations of the Indian Ocean, it does not include Red Sea overflow because of the relatively coarse resolution. The global HYCOM model also does not contain the channels at the north of the Tadjura Rift.

Within the constraints of our computational resources, one year data of salinity, temperature and horizontal velocities was downloaded from http://hycom.rsmas.miami.edu/dataserver/. The data is employed to provide initial and boundary conditions for the high-resolution regional model (Fig. 10). The numerical simulation is integrated for 345 days (from January 1st 2007 to December 15th 2007). The nested simulation is conducted on 64 processors and take approximately 15 days of wall clock time for a simulation time of one year. Since this is a whole year simulation, seasonality of the overflow needs to be taken into account. Matt and Johns, 2007 described that the Red Sea overflow nearly shuts down for three months in the summer. Therefore, the relaxation of the overflow water has been stopped between 165 and 260 days (i.e. between June 15 and September 20). We employ 50 km of the east part of the domain as a buffer zone (between 47.5°E and 48°E). Barotropic and baroclinic velocities, temperature and salinity fields of the global model are relaxed to the regional model in this area. The dense Red Sea overflow is released similar to the idealized cases using a relaxation region at the northern side. Temperature and salinity profiles are relaxed toward profiles taken from the REDSOX-1 observations at the Bab el Mandeb Strait using a relaxation time of thirty minutes.

There are two cyclones and an anticyclone at $z = -700$ m at the initial time, January 1, 2007 (Fig. 10), when RSOW is first released into the domain. Monthly snapshots of the salinity field are shown in Fig. 11. On January 15, the overflow just passes the Tadjura Rift and a basin-wide cyclone dominates the interior (Fig. 11(a)). By February 15, the overflow becomes a shelf-attached undercurrent and reaches to 46°E, where it separates from the boundary and flows into the interior (Fig. 11(b)). The cyclonic flow in the western GOA at this time is caused partly by the start-up of the RSOW outflow and partly by the arrival of a cyclone from the central GOA that can be seen in Fig. 11(a). It is clearly seen that the overflow is advected between this cyclone and the approaching anticyclone to the east. By March 15 the overflow has been transported around the northern rim of the anticyclone and reaches the northern boundary, where it begins to be swept back into the interior again (Fig. 11(c)). Entrance of a strong cyclone into the domain can be seen at the east side by April 15 (Fig. 11(c)). This eddy further mixes the RSOW in the GOA interior and leads to an enhanced

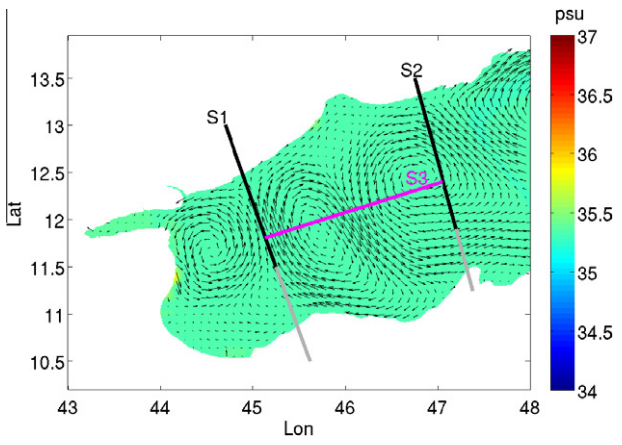

Fig. 10. Initial (January 1st 2007) salinity and velocity fields from global HYCOM simulation at depth = −700 m. Three sections across the outflow (S1, S2 and S3) are also used to compute the transport.

southern boundary current that exports RSOW out of the domain at 48°E. When the cyclone reaches the middle of the domain, the overflow waters in the western GOA are wrapped around its southern rim and transported into the interior again along 48°E (Fig. 11(e) and (f)).

On July 15, the cyclone moves further west and reduces in size (Fig. 11(g)), while a strong anticyclone enters from the east. Note that the source of the overflow is shut down at this time. On August 15, the cyclone moves southwestward and strengthens, and transports the overflow waters along the southern boundary (Fig. 11(h)), so that by September 15 there is only a weak signature of the RSOW remaining in the western GOA.

In October the outflow is turned on again and initially proceeds as a western/southern boundary current (Fig. 11(j) and (k)) before being swept into the interior by the cyclone/anticyclone pair evident in Fig. 11(k). The details of the eddy development in the domain and their interaction with the RSOW cannot be fully revealed with monthly snapshots, but these snapshots give an idea of the strength and complexity of the eddy field and its important role in the RSOW dispersion and export from the western GOA.

To assess how the eddies affect the mean distribution of RSOW in the Gulf, one-year-averaged salinity and velocity fields are computed from the simulation at the overflow depth (Fig. 12). It is clearly seen that the eddies do not homogenize the RSOW in the Gulf; there is still a concentration of Red Sea waters along the southern rim of the basin and an associated mean southern boundary current. The same basin-wide cyclonic circulation occurs as seen in the idealized experiments, although it is somewhat stronger due to the dominance of cyclonic eddy features in this one year experiment compared to anticyclones. Note that this broad scale cyclonic circulation is not present in the initial conditions (Fig. 10).

In summary, the overflow is mostly transported along the southern boundary throughout the whole year. Some of the overflow water surround GOA eddies and are advected into the interior of the GOA. However, it is clear that the favorable pathway of the overflow is as a shelf-attached boundary current. As in the idealized experiments, we conclude that interaction of multiple vortices with the overflow in the real GOA eddies simulation results in strong filamentation of the RSOW in the GOA and enhances mixing of the RSOW. The transport of the overflow in the boundary current and into the interior is episodic and depends on the strength and position of GOA eddies.

Fig. 13 displays the vertical salinity structure at Lon = 46°E for observation and nested model results. The salinity field observed during the REDSOX-I cruise in winter 2001 is shown in Fig. 13(a). The shelf attached RSOW can be seen at the southern side of the GOA (Lat ≈11°N). There are numerous salt patches in the interior because of stirring due to the GOA eddies. Bower et al., 2002 concluded that the Red Sea water salinity is much reduced due to stirring at this section by the two cyclones and an anti-cyclone observed during the cruise. Fig. 13(b) shows the model initial condition obtained from the HYCOM output. Note that the colorbar is different compared to the one used for the observed section. The initial condition does not contain any RSOW and it is clearly seen that the salinity in the interior is much fresher than observed. Figs. 13(c) and (d) display the modeled salinity field on July 15 and December 15, after approximately 6 months and 12 months of model integration, respectively. Salt patches due to the lateral stirring by eddies can be seen, analogous to those in the observations, especially in Fig. 13(c). The average salinity in the GOA interior remains lower than observed due to the initial condition; however, the interior field becomes more well-mixed as the integration proceeds and the salinity values are becoming comparable to those in the observations.

The transport of the Red Sea overflow through different sections is plotted in Fig. 14. There are two coast to coast sections, S1 and

Author's personal copy

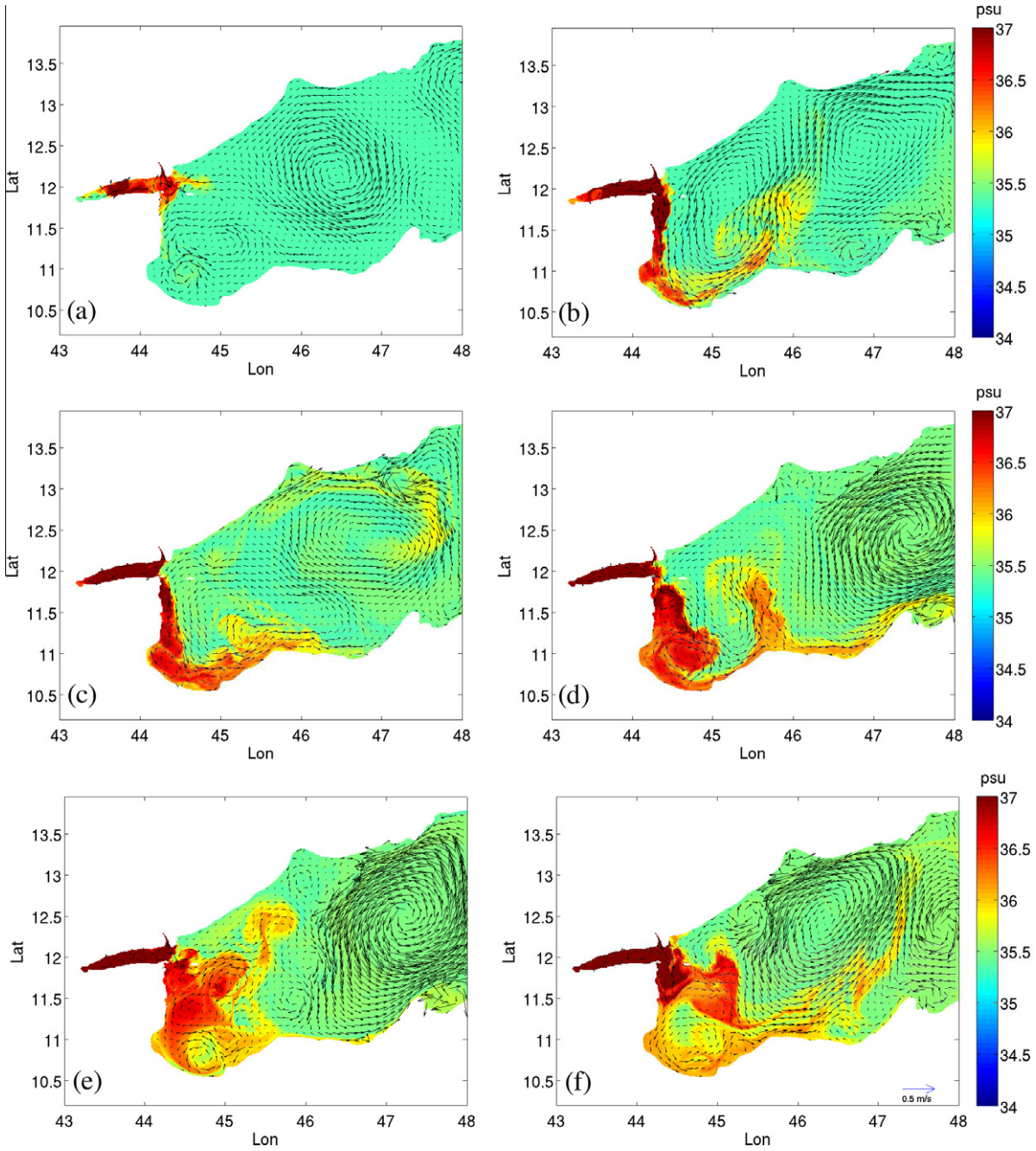

Fig. 11. 700 m horizontal sections for salinity field and velocity vectors at time = January 15 (a), February 15 (b), March 15 (c), April 15 (d), May 15 (e), June 15 (f). continued. Time = July 15 (g), August 15 (h), September 15 (i), October 15 (j), Novenber 15 (k), December 15 (l).

S2, and a cross section, S3 between S1 and S2 (Fig. 10). S1 and S2 are also separated into two parts. The first parts of these sections start from Somali coast and end around 80 km offshore (gray lines in S1 and S2) and the second parts are the rest of the S1 and S2 (black lines). Transports of the overflow across the gray lines provide a measure of the overflow water carried along the southern boundary, while transports across the black lines represent the interior transport of the overflow. Transports through section S3 (magenta line) represent the meridional transport of the overflow water between/through GOA eddies. Since the initial conditions from HYCOM model are fresher than the initial conditions in the previous idealized cases, mixing of the overflow with the ambient water results in lower average salinities. Thus, the threshold salinity used for defining the RSOW is reduced to a value of 35.8 psu from 36.5 psu. To exclude the mixed layer salinity values, we also take into account that salinity value must be at 200 m and/or lower than the surface. In the first 28 days, the RSOW transport through the southern part of section S1 is zero since the overflow has not arrived, yet. It then starts to increase and the mean transport value is 1.05 Sv. Maximum transport is around 6 Sv when the boundary current is also enhanced by a strong cyclone in the domain (Fig. 11(h)). The overflow is shut down between days 165 and 260, thus the transport decreases after 240 days and it becomes zero after 270 days. After that day, the south transport increases (blue line in Fig. 14(a)) since GOA eddies carries the overflow water (Fig. 11(l)). The total volume of the overflow through the boundary undercurrent is around 28.1×10^{12} m^3 at S1, while in the northern part, where eddies are dominant, it is around 7.9×10^{12} m^3. Thus,

Author's personal copy

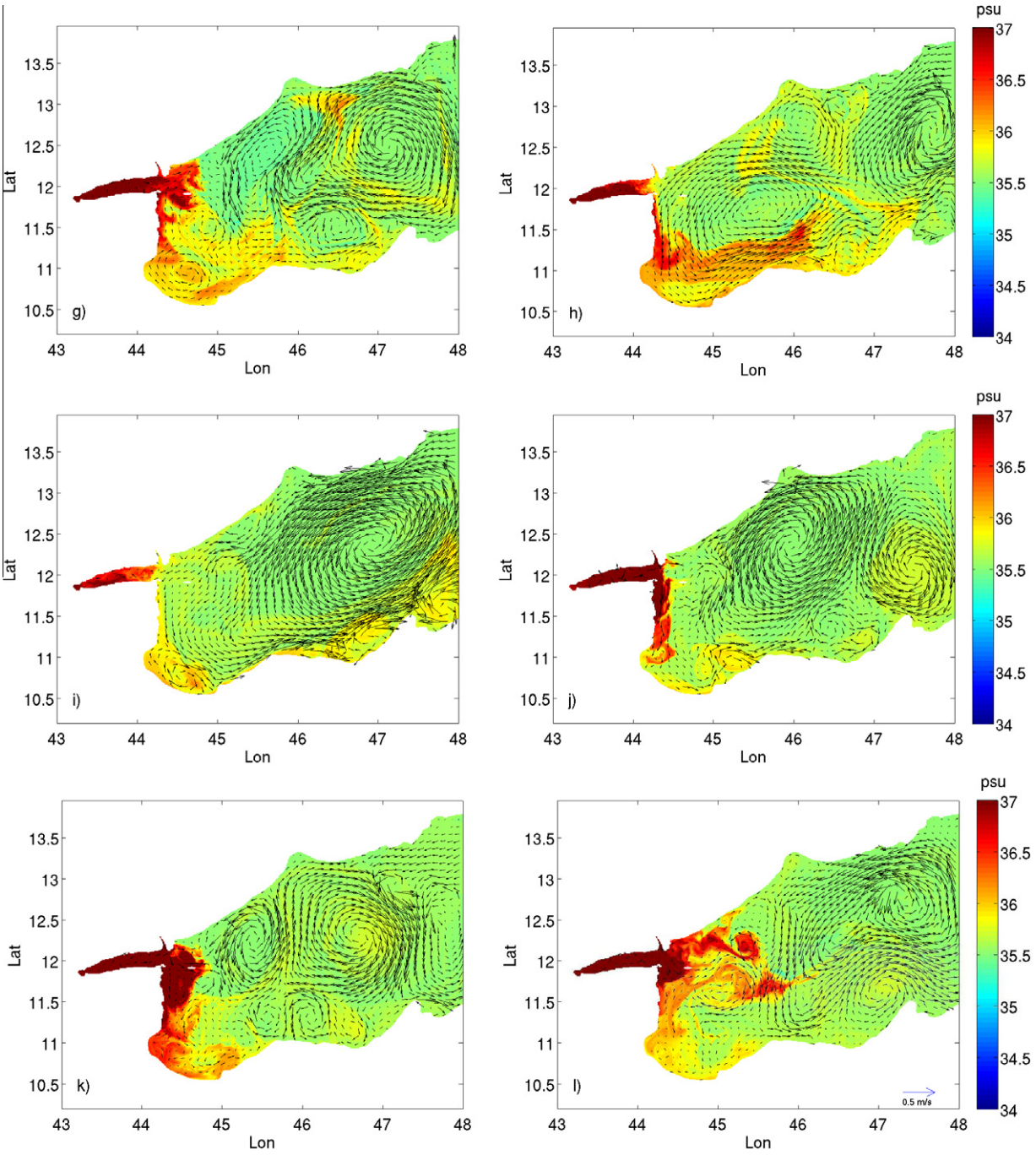

Fig. 11 (*continued*)

the total volume at Section 1 is 36×10^{12} m^3. Section 2, S2, is the eastern section and it is also separated into two components. Maximum transport at the south part of S2 is around 8.2 Sv which indicates entrainment in the overflow from S1 to S2. However total overflow volume at the shelf-attached current drops to 16.14×10^{12} m^3 while the total overflow volume through GOA eddies increases to 11.25×10^{12} m^3. We conclude that at the western part of the GOA the overflow is mostly carried by the shelf-attached current (78% of the total volume), then it decreases to 58.9% at the eastern part of the GOA. The volume of the overflow through GOA eddies increases from 22% of the total volume at the S1 to 41.1% of the total volume at the S2. Total volume at the Section 3, S3, is around 6.23×10^{12} m^3. This means that there is a net transport of the overflow from boundary current to the interior of the GOA domain.

The eastward transport of the overflow between 44.5°E and 47.5°E is also depicted in the form of Hovmöller diagram in Fig. 15. There are two strong events that increase the transport: one is at the beginning of June and the other is at the beginning of September. The transport of the overflow goes up to 3 Sv and 6 Sv, respectively in these events. These events can be also seen in Fig. 14. The first event is probably due to the basin size GOA cyclone in Fig. 11(f). The cyclone pushes the overflow, thus the transport increases. Around 190 days, transport of the overflow is negative at the east of 46.5°E due to anticyclone entered the domain (Fig. 11(g)). Since there is a strong cyclone in the GOA

Author's personal copy

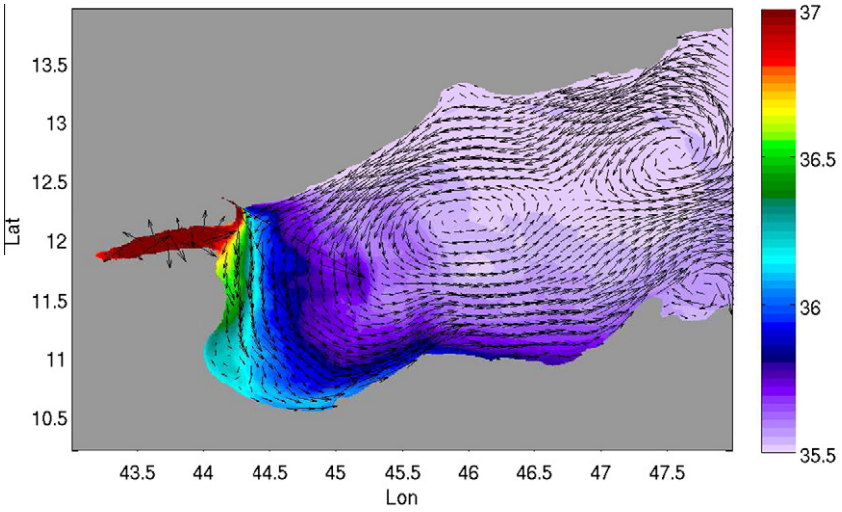

Fig. 12. (a) One year time-averaged salinity field and velocity vectors at $z = -700$ m horizontal section.

(Fig. 11(g)) at the beginning of September, the RSOW transport increases up to 6–7 Sv and the RSOW is carried away to the east. This is a very large amount of transport for the Red Sea overflow. It is known that the mean overflow transport is around 1 Sv (Fig. 8). A volume budget is computed to investigate the situation. The total RSOW volume exported from the model domain for the first 220 days is around 6.2×10^{12} m^3 at 47.5°E. However, the total amount of the overflow sank is around 14.2×10^{12} m^3 (1 [Sv] × 165 [days] × 86400 [s], note that the volume is computed for only 165 days since the overflow is shut down between 165 days and 220 days) which means that less than half of the overflow has left the domain. However, the total RSOW volume which left the domain between 220 days and 270 days is approximately 12.1×10^{12} m^3 at 47.5°E. It is evident that the overflow water leaves the western half of the GOA in less than two months. It is clear that the Red Sea overflow is not a steady current that leaves the GOA at a steady flow rate. On the contrary, it exits the Gulf of Aden like patches of Red Sea water due to presence of eddies and this happens as a burst in less than 50 days.

5. Discussion

The simulation with realistic GOA eddies raises several questions: (i) Why is the RSOW transport at the end of the domain (west half of the GOA) an order of magnitude greater than the transport at the beginning of the domain (BAM)? (ii) Can this be related to entrainment? (iii) What are the direct and/or indirect effects of the GOA eddies on such transport increase?.

To answer these questions, it is instructive to consider the following ideas. Let's consider the overflow as a control volume, with a total volume of V_{RSOW}, driven by the inflow at Section 1(Fig. 16), with transport Q_{in} across area A_{in} and speed U_{in}, $Q_{in} = A_{in}U_{in}$, and exiting the domain of interest at Section 3 with transport Q_{out} across area A_{out} and speed U_{out}, $Q_{out} = A_{out}U_{out}$. In the present study, Q_{in} corresponds to BAM while Q_{out} to the end of computational domain at 47.5°E. If one assumes that the overflow is isolated from its surroundings (adiabatic), and simply adjusts to the geometrical changes while maintaining a steady state, it follows that $Q_{out} = Q_{in}$. Furthermore, noting that the area of the BAM is much smaller than that of GOA, $A_{in} \ll A_{out}$, one may conclude that on average $U_{out} \ll U_{in}$.

Nevertheless, there are three factors that will change this simple consideration, namely entrainment by the overflow, seasonality of inflow at BAM and the possible influence of the GOA eddies. Including the entrainment transports Q_E, Q_e and temporal variability of the inflow and outflow transport, the overflow volume balance can be written as

$$\left(\frac{dV}{dt}\right)_{RSOW} = Q_{in}(t) - Q_{out}(t) + Q_E(t) + Q_e(t), \tag{2}$$

where Q_E is the vertical shear-induced entrainment during descent from BAM and Q_e is the possible entrainment induced by GOA eddies. Fig. 17(a) displays $(dV/dt)_{RSOW}(t)$, $[Q_{in}(t) - Q_{out}(t)]$ and $[Q_{Tadjura}(t) - Q_{out}(t)]$ during the 120 days of the realistic simulation. The difference between $(dV/dt)_{RSOW}(t)$ and $[Q_{in} - Q_{out}(t)]$ in Fig. 17(a) is balanced by the total entrainment, according to Eq. (2). Based on insight from our previous studies, we will assume that most of the entrainment $Q_E(t)$ occurs within the northern and southern channels. As such, by taking Section 2(Fig. 16) at exit from these channels in the Tadjura Rift, most of the Q_E will be included in the mass budget (2). This is confirmed in Fig. 17(a), in that $[Q_{Tadjura}(t) - Q_{out}(t)]$ is in better agreement with $(dV/dt)_{RSOW}(t)$ than $[Q_{in}(t) - Q_{out}(t)]$. The remaining differences are due to entrainment that takes place between Tadjura rift and 47.5°E. The main point is that the large fluctuations in the eastward RSOW transport cannot be associated with entrainment volume flux. Fig. 17(b) shows that $Q_{out}(t)$ changes independently from $Q_{in}(t)$, in fact it is largest when $Q_{in} = 0$ in the summer. Thereby, the only remaining factor is the influence of GOA eddies. Fig. 17(c) shows the mean relative vorticity in the GOA area and it can be clearly seen that the episodic events of the RSOW transport are correlated to the eddies in the GOA. Strong cyclone (positive vorticity) pushes the RSOW out of the domain where anticyclone (negative vorticity) keeps the RSOW in the GOA area. Given that the large fluctuations in $Q_{out}(t)$ can now be totally attributed to GOA eddies, we note that the azimuthal speed of the cyclonic GOA eddies, U_{eddy}, can be as high as 0.5 m/s, which is close to U_{in}. Therefore, we put forth that

$$Q_{out} \gg Q_{in} \quad \text{since} \quad U_{eddy} \approx U_{out} \approx U_{in} \quad \text{and} \quad A_{out} \gg A_{in}. \tag{3}$$

Fig. 18(a) shows that U_{out} can indeed be close to U_{in}, in particular coinciding with the period of the cyclone in September (but somewhat reduced by coastal effects). The discontinuities in U_{out} arise when there is no RSOW passing across the outflow section during these particular periods. Fig. 18b clearly shows that $A_{out} \gg A_{in}$ in that the stirring by the eddies leads to branching of the RSOW from the coast and increases the area of the RSOW. Combined with high azimuthal velocities of GOA eddies, one arrives at $Q_{out} \gg Q_{in}$. This is sustainable as long as supply of RSOW west of GOA cyclones lasts,

Author's personal copy

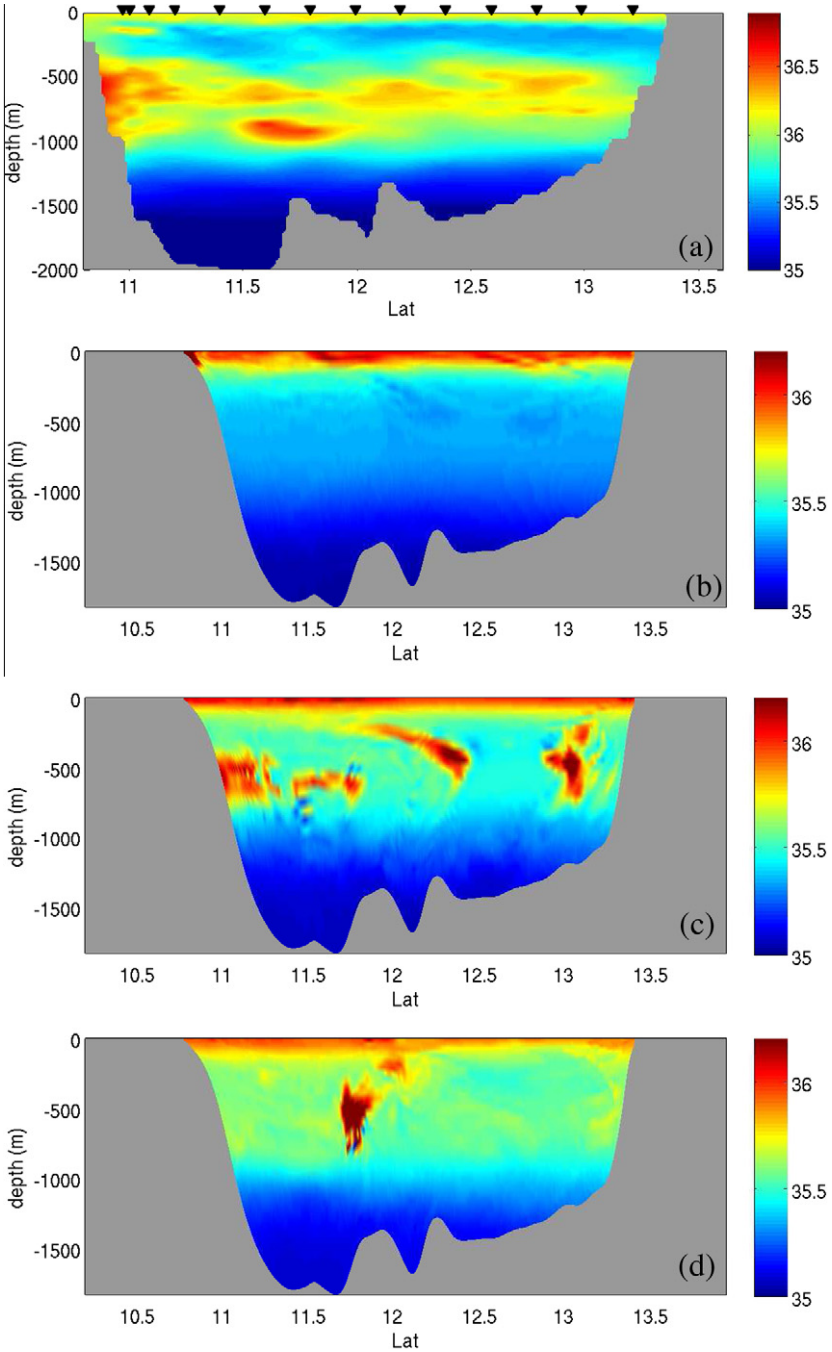

Fig. 13. Vertical sections for salinity field at Lon = 46°E: (a) REDSOX-I data interpolated using the Ocean Data View (`http://odv.awi.de/`) with DIVA (`http://modb.oce.ulg.ac.be/projects/1/diva`) grid interpolation. Station locations are shown at top. (b) Modeled initial salinity field taken from the HYCOM model. (c) The modeled salinity field on July 15. (d) The modeled salinity field on December 15.

thereby sometimes leading to disruptions in RSOW to the east of GOA eddies, and the episodic nature of the oscillations in Fig. 14.

One can wonder how the results above, obtained from RSOW volume budget, might be different if we look at the RSOW salt budget. One year simulation might not be sufficient to reach the quasi-steady averaged salinity in the western GOA. Fig. 19 displays the total RSOW volume and salt volume in the GOA. First, it is clearly seen that the total volume and salt volume have the same tendency. We expect this since the Red Sea overflow is mainly salinity-driven. Second, salt storage does not reach a steady value and it increases up to September. However, the strong cyclone at end of summer discharges all the RSOW as it was described above. We might conclude that the averaged salinity in the GOA might not become steady-state due to the cyclones in the GOA and seasonality of the Red Sea overflow.

6. Summary and conclusion

The RSOW can be traced as far south as the Agulhas Current. While entrainment by shear-induced mixing significantly modifies water mass properties of the RSOW, another dynamical obstacle before joining the Indian Ocean circulation is set by the mesoscale eddy field in the GOA. GOA eddies form either by retroflection of

Author's personal copy

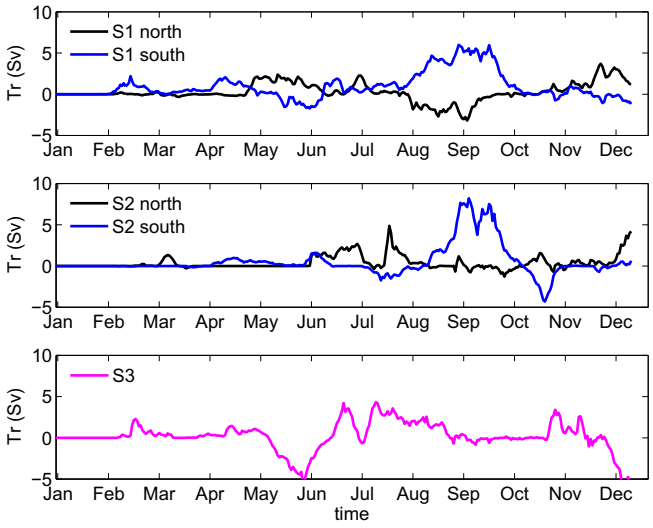

Fig. 14. Transport of the Red Sea overflow water (RSOW defined as $S > 35.7$ psu where $z < -200$ m) at sections S1, S2 and S3 (for the locations of the sections see Fig. 10).

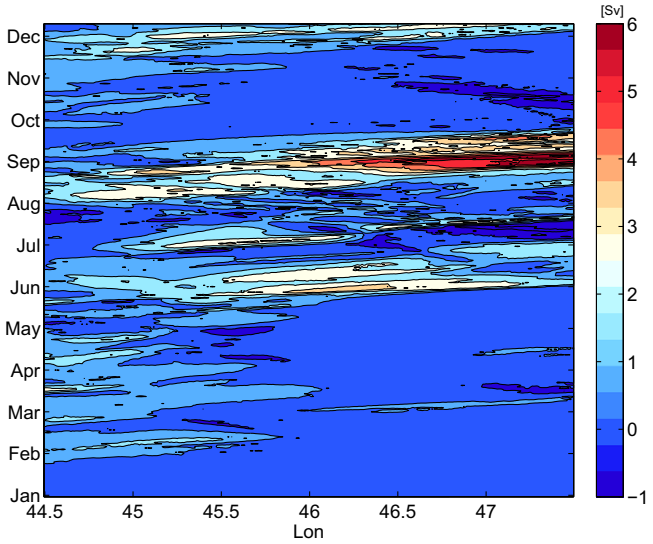

Fig. 15. Hovmoller diagram of the eastward RSOW transport (Sv) in time. RSOW is defined as $S > 35.7$ psu and the transport is computed over the entire cross section from bottom to $z = -200$ m.

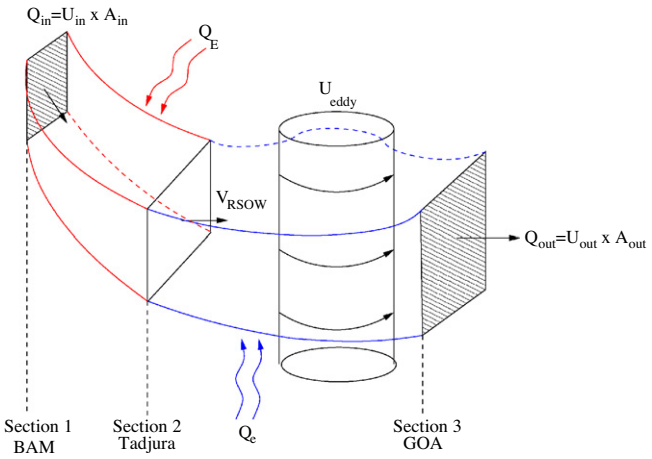

Fig. 16. Schematic depiction of the notation introduced for the pathways of RSOW from BAM to GOA.

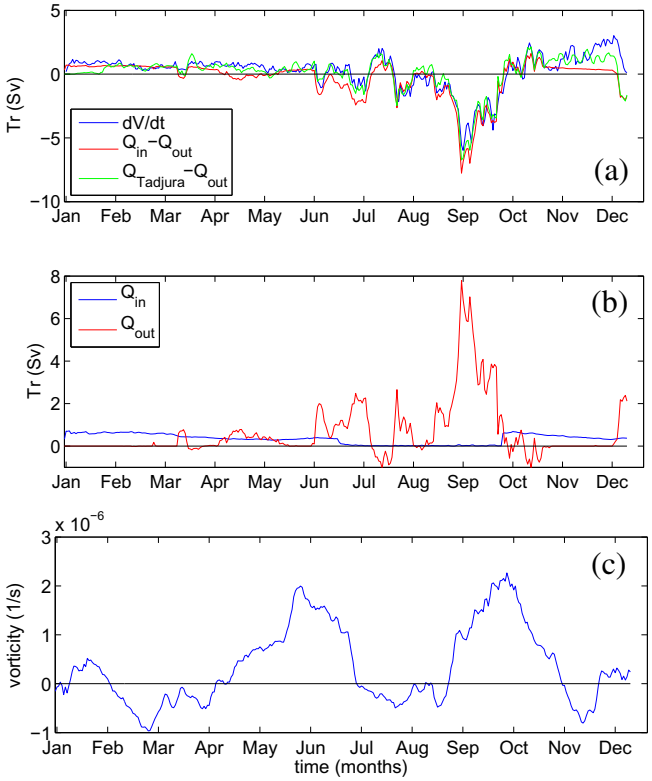

Fig. 17. (a) Temporal evolutions of $(dV/dt)_{RSOW}$, $Q_{in}-Q_{out}$ and $Q_{Tadjura}-Q_{out}$. (b) Inflow transport Q_{in} at the BAM and outflow transport Q_{out} at Lon = 47.5°E. (c) Space-averaged relative vorticity in the GOA area ($45.5 \leqslant x \leqslant 47.5$°E).

the Somali Current or westward propagating Rossby waves generated around Arabian Sea. Since they are deep-reaching vortices, they can influence the overflow equilibrated at intermediate depths.

In this study, we attempt to improve our understanding of the interaction between the Red Sea overflow and GOA eddies. We employ an expanded version of the model used in Ilıcak et al., 2008a. A set of three idealized experiments is conducted with different initial conditions. These include the overflow without any eddies, an idealized cyclone interacting with the overflow and an idealized anticyclone interacting with the overflow.

Analysis of the pathways, transport and mixing of the overflow yields the following conclusions. In the first idealized experiment, the overflow is released without any eddies (the case **O**). The overflow follows the southern boundary and becomes a shelf-attached boundary current. The overflow induces a cyclone due to the potential vorticity constraint. The **O + C** case consists of the overflow with an idealized cyclone. Two new eddies form after the initial cyclone dissipates. The favorable pathway is still as a boundary undercurrent. The last idealized experiment, **O + A**, initializes the overflow with an idealized anticyclone. The overflow pushes the anticyclone towards the east of GOA. The eddy acts as a barrier and does not let the overflow penetrate to the east. In this case, the overflow water is mostly transported by the advection due to the anticyclone rather than shelf-attached boundary current. We also look at T/S properties of the overflow for different cases. In the **O + C** case, the presence of the initial cyclone and two other eddies stir the overflow. It is evident that lateral mixing takes place in the **O + C** case. In the last idealized case, the anticyclone barrier forces the overflow to mix laterally. It is clear in both experiments

Author's personal copy

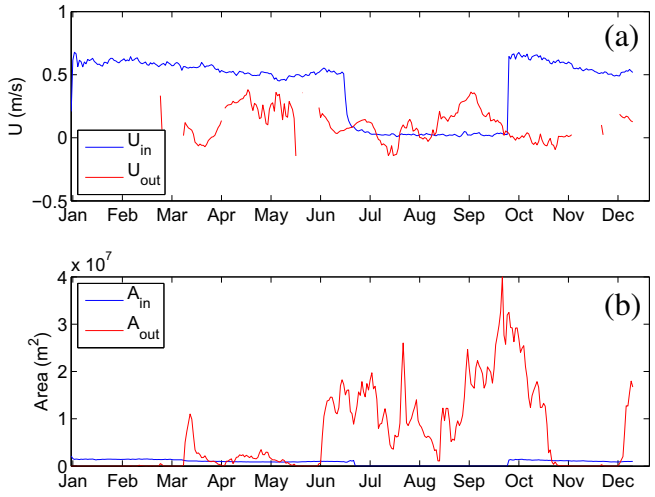

Fig. 18. (a) Space-averaged velocity U_{in} of the RSOW at the BAM and U_{out} at Lon = 47.5°E. (b) total area of the RSOW at the BAM and exit of the GOA.

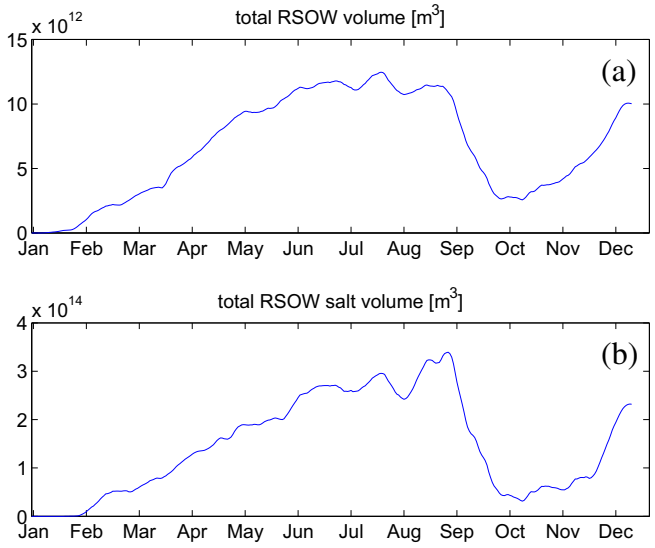

Fig. 19. (a) Total volume ($\int dxdydz$) of the RSOW in the GOA. (b) Total salt volume ($\int Sdxdydz$) of the RSOW in the GOA. RSOW is defined as $S > 35.7$ psu and total volume is computed over the entire cross section from bottom to $z = -200$ m.

with imposed eddies that the overall dilution of the Red Sea overflow water is greater than in the pure overflow case.

In order to incorporate a realistic sequence of GOA eddies, we employed output from a global HYCOM as initial and boundary conditions for the regional model. The global HYCOM could not be directly used for this study, since even with 1/12° horizontal resolution, it entirely lacks RSOW in GOA, implying under-resolved exchange flow with the Red Sea domain. The regional model is then integrated for one year, including a simple representation of the seasonality of RSOW (the overflow is shut down at BAM in the summer). Our main finding is that GOA eddies can modulate the transport of RSOW significantly such that RSOW leaves the western half of the GOA in short episodic bursts with transports reaching 6 Sv, which is an order of magnitude larger than the steady transport of RSOW out of the channels. Such enhancement of RSOW transport within the GOA is shown to be induced by cyclonic GOA eddies, while anticyclonic eddies tend the block the eastward propagation of the RSOW, as in idealized experiments. GOA eddies have speeds comparable to RSOW during its origin, namely the descent from the BAM Strait, but cyclonic eddies propel RSOW, that has accumulated near the juncture of Tadjura Rift to GOA (about 44.5–45°E), eastward by acting over a much larger cross-sectional area when compared to that of the BAM, resulting in a rapid discharge of RSOW from the western part of the GOA.

Future studies should focus on longer term simulations in an extended domain and more realizations of GAO eddy interactions with the RSOW, in order to better reveal how rapid discharge of RSOW by cyclones, and accumulation inside GOA by anticyclones influence the RSOW transport into the Indian Ocean basin. It is also of interest to pursue applications of concepts based on dynamical systems theory on the transport of RSOW by the eddies. A careful investigation of the amount of mixing and entrainment induced by the strain field associated with mesoscale eddies in RSOW is probably worthy of investigation as well.

Acknowledgments

We are grateful for the support of National Science Foundation Grant OCE 0620661. We thank Marcello G. Magaldi and David S. Nolan for their help in different phases of this study.

References

Aiki, H., Takahashi, K., Yamagata, T., 2006. The Red Sea outflow regulated by the Indian monsoon. Cont. Shelf Res. 26 (August), 1448–1468.
Al Saafani, M.A., Shenoi, S.S.C., Shankar, D., Aparna, M., Kurian, J., Durand, F., Vinayachandran, P.N., 2007. Westward movement of eddies into the Gulf of Aden from the Arabian Sea. J. Geophys. Res. (Oceans) 112 (November), 11004.
Beal, L.M., Ffield, A., Gordon, A.L., 2000. Spreading of red sea overflow waters in the indian ocean. J. Geophys. Res. 105, 8549–8564.
Bower, A.S., Fratantoni, D.M., Johns, W.E., Peters, H., 2002. Gulf of Aden eddies and their impact on Red Sea Water. Geophys. Res. Lett. 29 (November), 21-1.
Bower, A.S., Johns, W.E., Frantantoni, D.M., Peters, H., 2005. Equilibration and circulation of Red Sea outflow water in the western Gulf of Aden. J. Phys. Oceanogr. 35, 1963–1985.
Candela, J., 2001. Mediterranean water and global circulation. In: Ocean Circulation and Climate. Academic Press, San Diego, California, pp. 419–429.
Canuto, V.M., Howard, A.M., Cheng, Y., Dubovikov, M.S., 2001. Ocean turbulence. Part I: One-point closure model momentum and heat vertical diffusivities. J. Phys. Oceanogr. 31, 1413–1426.
Carton, X.J., Flierl, G.R., Polvani, L.M., 1989. The generation of tripoles from unstable axisymmetric isolated vortex structures. Europhys. Lett. 9 (June), 339.
Chang, Y.S., Özgökmen, T.M., Peters, H., Xu, X., 2008. Numerical simulations of the red sea outflow using hycom and comparison with redsox observations. J. Phys. Oceanogr. 38/2, 337–358.
Cummings, J.A., 2005. Operational multivariate ocean data assimilation. J. R. Meteorol. Soc., 131.
Ezer, T., 2006. Topographic influence on overflow dynamics: idealized numerical simulations and the faroe bank channel overflow. J. Geophys. Res. 111 (February), 2002.
Fratantoni, D.M., Bower, A.S., Johns, W.E., Peters, H., 2006. Somali current rings in the eastern Gulf of Aden. J. Geophys. Res. 111 (September), 9039.
Girton, J.B., Sanford, T.B., Käse, R.H., 2001. Synoptic sections of the denmark strait overflow. Geophys. Res. Lett. 28, 1619–1622.
Ilıcak, M., Özgökmen, T.M., Peters, H., Baumert, H.Z., Iskandarini, M., 2008a. Performance of two-equation turbulence closures in three-dimensional simulations of the Red Sea overflow. Ocean Modell. 24, 122–139.
Ilıcak, M., Özgökmen, T.M., Peters, H., Baumert, H.Z., Iskandarini, M., 2008b. Very large Eddy simulation of the Red Sea Overflow. Ocean Modell. 20, 183–206.
Jackett, D.R., McDougall, T.J., 1995. Minimal adjustment of hydrostatic profiles to achieve static stability. J. Atmos. Oceanic Tech. 12, 381–389.
Macrander, A., Käse, R.H., Send, U., Valdimarsson, H., Jónsson, S., 2007. Spatial and temporal structure of the Denmark Strait Overflow revealed by acoustic observations. Ocean Dyn. 57 (April), 75–89.
Marchesiello, P., McWilliams, J.C., Shchepetkin, A., 2001. Open boundary conditions for long-term integration of regional oceanic models. Ocean Modell. 3, 1–20.
Matt, S., Johns, W.E., 2007. Transport and entrainment in the red sea outflow plume. J. Phys. Oceanogr. 37, 819–836.
Morcos, S.A., 1970. Physical and chemical oceanography of the Red Sea. Oceanogr. Mar. Biol. Ann. 8, 73–202.
Morel, Y., McWilliams, J., 1997. Evolution of isolated interior vortices in the ocean. J. Phys. Oceanogr. 27 (May), 727–748.
Murray, S.P., Johns, W., 1997. Direct observations of seasonal exchange through the Bab el Mandab Strait. Geophys. Res. Lett..
Özgökmen, T.M., Johns, W.E., Peters, H., Matt, S., 2003. Turbulent mixing in the red sea outflow plume from a high-resolution nonhydrostatic model. J. Phys. Oceanogr. 33, 1846–1869.

Author's personal copy

Peters, H., Johns, W.E., 2005. Mixing and entrainment in the red sea outflow plume. Part II: Turbulence characteristics. J. Phys. Oceanogr. 35, 584–600.
Peters, H., Johns, W.E., 2006. Bottom layer turbulence in the red sea outflow plume. J. Phys. Oceanogr. 36, 1763–1785.
Peters, H., Johns, W.E., Bower, A.S., Fratantoni, D.M., 2005. Mixing and entrainment in the red sea outflow plume. Part I: Plume structure. J. Phys. Oceanogr. 35, 569–583.
Roman, R., Lutjeharms, J., 2007. Red sea intermediate water at the Agulhas current termination. Deep Sea Res. Part I 54, 1329–1340.
Shchepetkin, A.F., McWilliams, J.C., 2005. The regional oceanic modeling system (roms): a split-explicit, free-surface, topography-following-coordinate oceanic model. Ocean Modell. 9, 347–404.
Spall, M.A., Price, J.F., 1998. Mesoscale variability in denmark strait: the PV outflow hypothesis. J. Phys. Oceanogr. 28, 1598–1623.